Sensing and Control on the Sphere

Peter Corke and Robert Mahony

Abstract The advantages of a spherical imaging model are increasingly well recognized within the robotics community. Perhaps less well known is the use of the sphere for attitude estimation, control and scene structure estimation. This paper proposes the sphere as a unifying concept, not just for cameras, but for sensor fusion, estimation and control. We review and summarize relevant work in these areas and illustrate this with relevant simulation examples for spherical visual servoing and scene structure estimation.

1 Introduction

In the last few years there has been growing interest in image processing operations performed on the sphere stemming from a number of important developments. Firstly, a wide perceptual field is important for robotic path planning and collision avoidance and led researchers to adopt, or develop, wide-angle viewing systems [5, 31, 34]. Secondly, the mathematical techniques for spherical imaging have matured, for example the unified imaging model [16], spherical scale-space [3] and spherical SIFT [18]. Thirdly, as purely vision-based navigation becomes possible the ambiguity between rotation and translation which is problematic in a perspective camera image can be overcome by using wide angle imagery. Finally, there is a biological inspiration from small flying insects which use very wide angle eyes, sometimes combined with gyroscopic sensors to perform complex navigation tasks [6].

Pose estimation, including both position and attitude estimation, is a key requirement for autonomous operation of robotic vehicles. For aerial and underwater robots, attitude estimation is especially important. Micro-Electro-Mechanical Sys-

Peter Corke
CSIRO ICT Centre, e-mail: peter.corke@csiro.au

Robert Mahony
Australian National University e-mail: robert.mahony@anu.edu.au

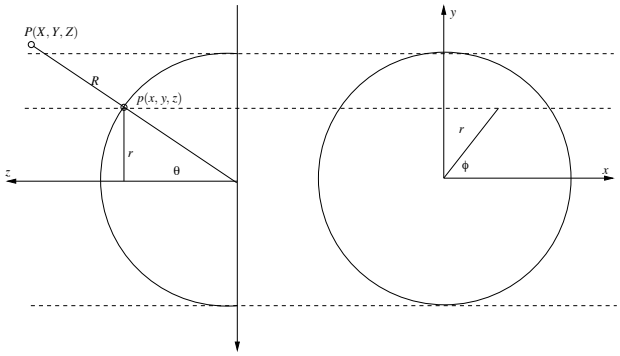

Fig. 1 The coordinate system. P is a world point, mapped to p on the surface of the unit sphere represented by the angles θ and ϕ.

tems (MEMS) technology has led to a range of low-cost and compact light-weight inertial measurement units that can be used to provide reliable measurements of angular velocity, direction of gravity and altitude. Sensors for magnetic field direction are also available. Good quality, lightweight and low-cost fisheye or catadioptric camera systems are available to provide additional information such as the orientation of vertical edges in the environment [28] or the plane of the horizon [6]. None of these sensors estimate full attitude, in SO(3), directly and it turns out that the attitude estimation problem is best tackled using sphere-based measurements.

Optical flow is an important low-level image cue that encodes both ego-motion and scene structure. We discuss the spherical optical-flow equation and its advantages for detecting key ego-motion parameters such as direction of motion. The optical flow equations can be inverted to create an image-based visual servoing (IBVS) system as well as a structure from motion estimator.

The next section, Section 2, derives the optical flow equation and image Jacobian for the sphere, and then in Section 3 we briefly recall the unified imaging model that can be used to create a spherical image from one or more cameras that could be perspective, fisheye or catadioptric. Section 4 describes sensor fusion on the sphere for the case of attitude and full-pose estimation. Section 5 inverts the optical flow equation to effect control on the spherical image plane and Section 6 outlines the advantages of the sphere for the structure from motion problem.

2 Spherical optical flow

As for the case of a perspective camera [21] we assume that the camera is moving with translational velocity $\mathbf{T} = (t_x, t_y, t_z)$ and angular velocity $\boldsymbol{\omega} = (\omega_x, \omega_y, \omega_z)$ in the camera frame. A world point, $\mathbf{P}$, with camera relative coordinates ${}^c\mathbf{P} = (X, Y, Z)^T$ has camera-relative velocity

$$ {}^c\dot{\mathbf{P}} = -{}^c\boldsymbol{\omega}_e \times {}^c\mathbf{P} + {}^c\mathbf{T}_e \tag{1} $$

which can be written in scalar form as

$$ \dot{x} = z\omega_y - y\omega_z + t_x \tag{2} $$
$$ \dot{y} = x\omega_z - z\omega_x + t_y \tag{3} $$
$$ \dot{z} = y\omega_x - x\omega_y + t_z \tag{4} $$

The world point P is projected, Figure 1, to p on the surface of the unit sphere

$$ x = \frac{X}{R},\ y = \frac{Y}{R}, \text{ and } z = \frac{Z}{R} \tag{5} $$

where the focal point is at the center of the sphere and the radial distance to the point is $R = \sqrt{X^2 + Y^2 + Z^2}$. The spherical surface constraint $x^2 + y^2 + z^2 = 1$ means that one of the Cartesian coordinates is redundant, and we will instead use a minimal spherical coordinate system comprising the angle of colatitude

$$ \theta = \sin^{-1} r,\ \theta = [0,\ \pi) \tag{6} $$

and the azimuth angle

$$ \phi = \tan^{-1} \frac{y}{x},\ \phi = [0,\ 2\pi) \tag{7} $$

yielding the point feature vector $\mathbf{f} = (\theta, \phi)$. Other spherical image features are possible such as lines or moments [36].

Taking the derivatives of (6) and (7) with respect to time and substituting (2) – (4) as well as

$$ X = Z\tan\theta\cos\phi,\ Y = Z\tan\theta\sin\phi. \tag{8} $$

we obtain, in matrix form, the polar optical flow equation

$$ \begin{bmatrix} \dot{\theta} \\ \dot{\phi} \end{bmatrix} = \mathbf{J}(\theta, \phi, Z) \begin{bmatrix} t_x\ t_y\ t_z\ \omega_x\ \omega_y\ \omega_z \end{bmatrix}^T \tag{9} $$

where

$$ \mathbf{J}(\theta,\phi,Z) = \begin{bmatrix} \frac{\cos(\phi)\cos^2(\theta)}{Z(t)} & \frac{\sin(\phi)\cos^2(\theta)}{Z(t)} & -\frac{\cos(\theta)\sin(\theta)}{Z(t)} & \vdots & -\sin(\phi) & \cos(\phi) & 0 \\ -\frac{\sin(\phi)\cos(\theta)}{Z(t)\sin(\theta)} & \frac{\cos(\phi)\cos(\theta)}{Z(t)\sin(\theta)} & 0 & \vdots & -\frac{\cos(\phi)\cos(\theta)}{\sin(\theta)} & -\frac{\sin(\phi)\cos(\theta)}{\sin(\theta)} & 1 \end{bmatrix} \tag{10} $$

is the image feature Jacobian or optical flow equation in terms of the *spherical* point feature $\mathbf{f} = (\theta, \phi)$.

There are important similarities to the Jacobian derived for projective cameras in polar coordinates [8,22]. Firstly, the constant elements 0 and 1 fall at the same place, indicating that colatitude is invariant to rotation about the optical axis, that azimuth angle is invariant to optical axis translation, but equal to optical axis rotation. As for all image Jacobians the translational sub-matrix (the first 3 columns) is a function

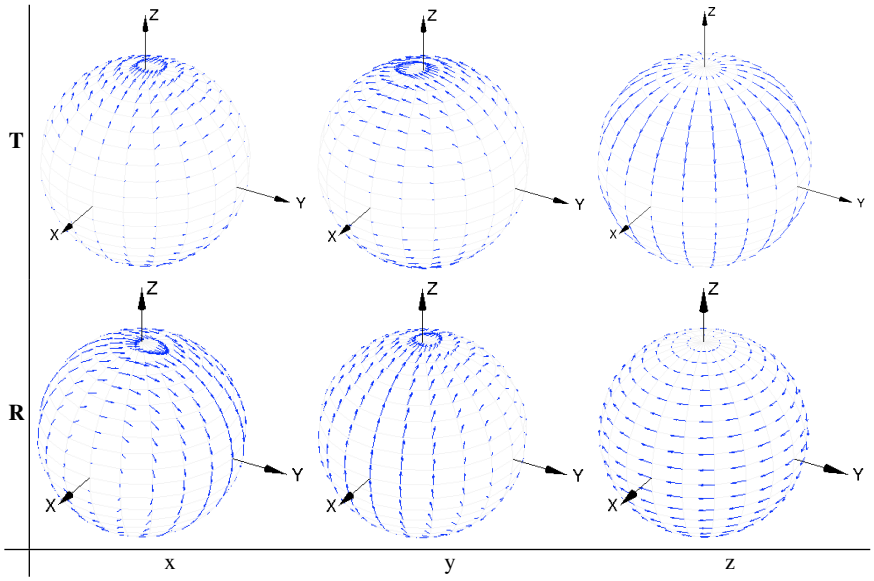

Fig. 2 Spherical optical flow patterns for canonical motion along and about x-, y- and z-axes.

of point depth $1/Z$. Note also that the Jacobian is not defined at the poles where $\sin\theta = 0$.

The optical flow patterns on the sphere, for canonical motions, are shown in Figure 2. We note the distinctly different flow patterns for each Cartesian velocity component. A perspective camera with its optical axis aligned with the z-axis has a field of view equivalent to a polar cap, and within that small region of the sphere we can see that the flow due to t_x and ω_y are close to indistinguishable, as are t_y and ω_x. This is a consequence of making a 2-DOF measurement (optical flow) of a 6-DOF phenomena (spatial velocity) leading to a null-space of order 4; in this some motions are linearly dependent (the indistinguishable flows) and some are unobservable (two are null at the pole).

We can also partition the Jacobian [10] into a translational and rotational part

$$\begin{bmatrix} \dot{\theta} \\ \dot{\phi} \end{bmatrix} = \frac{1}{Z}\mathbf{J}_t(\theta,\phi)\begin{bmatrix} t_x \\ t_y \\ t_z \end{bmatrix} + \mathbf{J}_\omega(\theta,\phi)\begin{bmatrix} \omega_x \\ \omega_y \\ \omega_z \end{bmatrix} \tag{11}$$

which is important for both control and structure estimation. For points at infinity the first term will be zero.

Optical flow on the sphere can be calculated using a range of approaches, either on the sphere, or on the camera's image plane and mapped to the sphere as discussed in the next section.

3 Mapping cameras to the sphere

Recent and growing interest in wide-angle viewing systems [5, 31, 34] has been driven by application need for path planning and collision avoidance and also the availability of new cameras. For instance high-quality glass fisheye lenses with just over a hemispherical field of view have been used by researchers for several years now, and lower-quality low-cost plastic fisheye lenses suitable for small aerial robots have also been investigated [33]. Reasonable quality, lightweight and or catadioptric camera systems are also available.

The unified model of Geyer and Daniilidis [16] provides a convenient framework to consider very different types of cameras such as standard perspective, catadioptric and many types of fisheye lens. The projection model is a two-step process and the key concepts are shown in Figure 3. Firstly, the world point P is projected to the surface of the unit sphere with a focal point at the center of the sphere. The center of the sphere is a distance m from the image plane along its normal z-axis. Secondly the point p is re-projected to the image plane m with a focal point at a distance l along the z-axis, where l is a function of the imaging geometry.

Commonly used mirrors have a parabolic or hyperbolic cross-section, and for these $l = \varepsilon$ the eccentricity of the conic section: $l = 1$ for a parabola and $0 < \varepsilon < 1$ for a hyperbola. This class of mirrors result in a *central* camera with a single effective viewpoint, that is, all rays in space intersect at a single point. Mirrors commonly used in robotics, for example [12,34], have an equiangular model and the viewpoint lies along a short locus (the *caustic*) within the mirror. In practice this difference in focal point is very small compared to the world scale and such mirrors are well

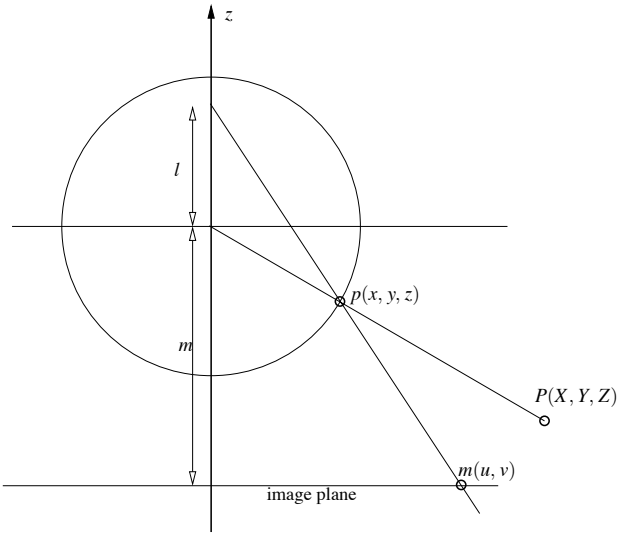

Fig. 3 Unified imaging model of Geyer and Daniilidis [16].

approximated by the central model. Subsequent work [39] showed that many fisheye cameras could also be included in this framework, generally with $l > 1$. For a perspective camera $l = 0$ and the first and second projection rays overlap.

We can invert the unified model and project an image, features or optical flow from a camera image plane (perspective, fisheye or catadioptric) to the sphere for subsequent processing. In [18] catadioptric and fisheye images were projected to the sphere for scale-space computation using a spherical equivalent of the Gaussian kernel. In [33] sparse optical flow was projected to the sphere for focus of expansion detection.

True spherical cameras are under development [25] but until they become a reality we must be content with partial spherical views from a camera, or a mosaic view from multiple cameras (such as the Point Grey Ladybug camera). The spherical framework allows the mapping of multiple cameras with different orientations and different fields of view and projection models to the sphere from their individual image planes, and this is shown schematically in Figure 4 (left).

In practice the various images are not obtained from exactly the same viewpoint, but from slightly offset viewpoints caused by the physical separation of the individual cameras and this leads to parallax error as shown in Figure 4 (right). This is problematic in areas of camera overlap and exacerbated when the inter-camera distances are significant compared to the distance to the point. It can be resolved, that is, the point projected to O if the range to P can be estimated which is a stereo vision problem between the cameras centered at C_1 and C_2.

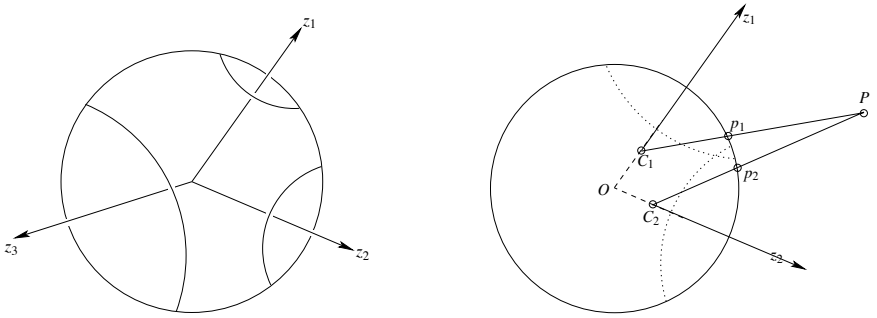

Fig. 4 (left) multiple camera views mapped to the sphere, (right) parallax on the sphere when camera centers, C_1 and C_2 are not coincident with the center of the sphere O.

4 Sensor fusion on the sphere

4.1 Attitude estimation

There is a considerable body of work on attitude reconstruction for robotics and control applications (for example the review [13]). A standard approach is to use extended stochastic linear estimation techniques [26]. An alternative is to use deterministic complementary filter and non-linear observer design techniques [1, 38]. [15]. The recent interest in small low-cost aerial robotic vehicles has lead to a renewed interest in lightweight embedded IMU systems [1, 23, 35]. For the low-cost light-weight systems considered, linear filtering techniques have proved extremely difficult to apply robustly [32] and linear single-input single-output complementary filters are often used in practice [9]. The integration of inertial and visual information is discussed in [11].

Gyroscopes provide an estimate of angular velocity, Ω, corrupted by an offset which leads to drift in attitude after integration. We can constrain the estimate by minimizing the error angle between a reference direction and its estimate on the sphere in the body-fixed-frame. To fully constrain the solution at least two non-collinear reference directions are required. Each of these directions and estimates can be projected to the surface of the sphere as shown in Figure 5 as small circles. One such reference direction can be obtained from the gravity field vector — the

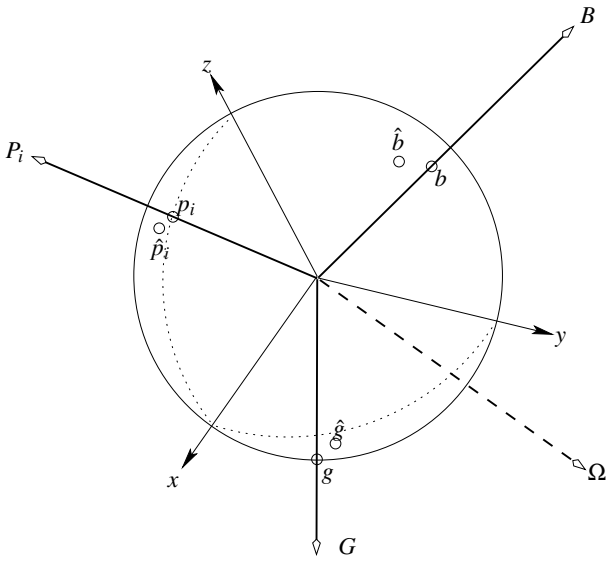

Fig. 5 Sensor integration on the sphere. The attitude of the body is indicated by the x-, y- and z-axes. The predicted and measured sensor vector projections are shown by small circles. Visual landmarks are also included.

the magnitude is irrelevant only its direction on the sphere is required. If the body is accelerating in the inertial frame this vector will be corrupted by inertial forces, however, for steady or hovering flight of a UAV the accelerometers approximately measure the gravitation field in the body-fixed-frame. Another reference direction can be provided by the Earth's magnetic field B at the location. Visual tracking of very distant feature points (at infinity) provide additional reference directions.

The natural framework to interpret these measurement is on the sphere in the body-fixed-frame of the mobile vehicle. Recent work in the development of non-linear observers for attitude estimation provides an ideal framework for the construction of robust and efficient attitude filters based on vector measurements on the sphere [2, 4, 29, 30, 37].

More formally the attitude estimation problem can be expressed in terms of sphere based measurements [29] using the matrix Lie-group representation of $SO(3)$ — the group of rotations associated with the attitude of a rigid-body. The attitude kinematics is described by

$$\dot{R} = R\,{}^{B}\Omega_{\times}. \tag{12}$$

where ${}^{B}\Omega$ is the body-fixed-frame angular velocity of the rigid-body and $[\,]_{\times}$ denotes the skew-symmetric matrix. Consider measurements from $n \geq 1$ sensors in the body-fixed frame $a_i \in S^2_B\ i = 1, 2, \ldots n$ each of which has an associated reference directions in the world frame $a_{0i} \in S^2_W$. These are expressed as vectors on the unit sphere in the inertial frame. Let $\hat{a}_i$ be the estimates of the sensor measurements in the body frame

$$\hat{a}_i = \hat{R}^{\top} a_{0i} \tag{13}$$

based on the estimated attitude $\hat{R}$.

The complementary observer proposed in [29] is

$$\dot{\hat{R}} = \hat{R}(\Omega_y - \hat{b} + \omega_{\text{mes}})_{\times} \tag{14}$$

$$\dot{\hat{b}} = -2k_I\,\omega_{\text{mes}} \tag{15}$$

$$\omega_{\text{mes}} = \sum_{i=1}^{n} k_i (a_i \times \hat{a}_i) \tag{16}$$

where Ω_y is the measured body-fixed-frame angular velocity obtained from the gyroscopes, $\hat{b}$ is the gyroscope bias, and $k_i \geq 0$. It is shown that the attitude estimate $\hat{R}$ will approach the true attitude R asymptotically. For implementation we use quaternions and the following algorithm:

1. Determine ω_{mes} from available sensor measurements according to (13) and (16)
2. Compute the quaternion velocity

$$\dot{\hat{q}} = \frac{1}{2}\hat{q} \otimes \mathbf{p}\left(\Omega_y - \hat{b} + k_P\,\omega_{\text{mes}}\right)$$

where $\mathbf{p}$ converts a vector to a pure quaternion and $\otimes$ represents quaternion (Hamiltonian) multiplication.

3. Integrate and renormalize the quaternion

$$\hat{q}_{k+1} = \hat{q}_k + \delta_t \dot{\hat{q}}$$
$$\hat{q}_{k+1} = \hat{q}_{k+1} / ||\hat{q}_{k+1}||$$

4. Update the gyroscope bias estimate

$$\hat{b}_{k+1} = \hat{b}_k + \delta_t \dot{\hat{b}}$$

The gains $k_i(t)$ can be set adaptively depending on confidence in particular sensors.

4.2 Pose estimation

Pose estimation, including both position and attitude estimation, is a key requirement for autonomous operation of robotic vehicles, especially aerial robots. Modern Global Positioning Systems (GPS) are have decreasing cost, weight, and energy consumption while increasing quality and functionality. Carrier phase doppler shift can be extracted from GPS signals to provide inertial frame velocity estimates of a vehicle's motion [19] and rotated into the body-fixed-frame based on an attitude estimate.

In the absence of GPS, due to denial or a multi-pathing environment, we can extract information about translational motion from the optical flow field. If optical flow due to rotational motion is estimated and subtracted, a process known as *derotation*, the remaining optical flow is due only to translation, corrupted with noise from the optical flow process itself and errors in the rotational estimate. A characteristic of the translational flow field is a focus of expansion on the sphere at the point defined by the vector $\mathbf{d}$ where $\mathbf{d} = \mathbf{t}/|\mathbf{t}|$. As discussed above the optical flow encodes translational motion with a scale uncertainty, that is $\mathbf{t}/Z$ not $\mathbf{t}$ can be identified. Expressed another way, the direction of motion is a unit vector through the focus of expansion on the sphere. A corresponding focus of contraction will be found at the antipodal point. Recent approaches to determining the focus of expansion from optical flow are [27].

5 Control on the sphere

Visual servoing is the use of information from one or more cameras to guide a robot so as to achieve a task [7, 21]. Image-Based visual servoing (IBVS) is a robust and efficient technique where the task is defined in terms of the desired view of the target and a control law is synthesized to move the camera toward that view. The goal is defined *implicitly* in the desired view. The pose of the target does not need to

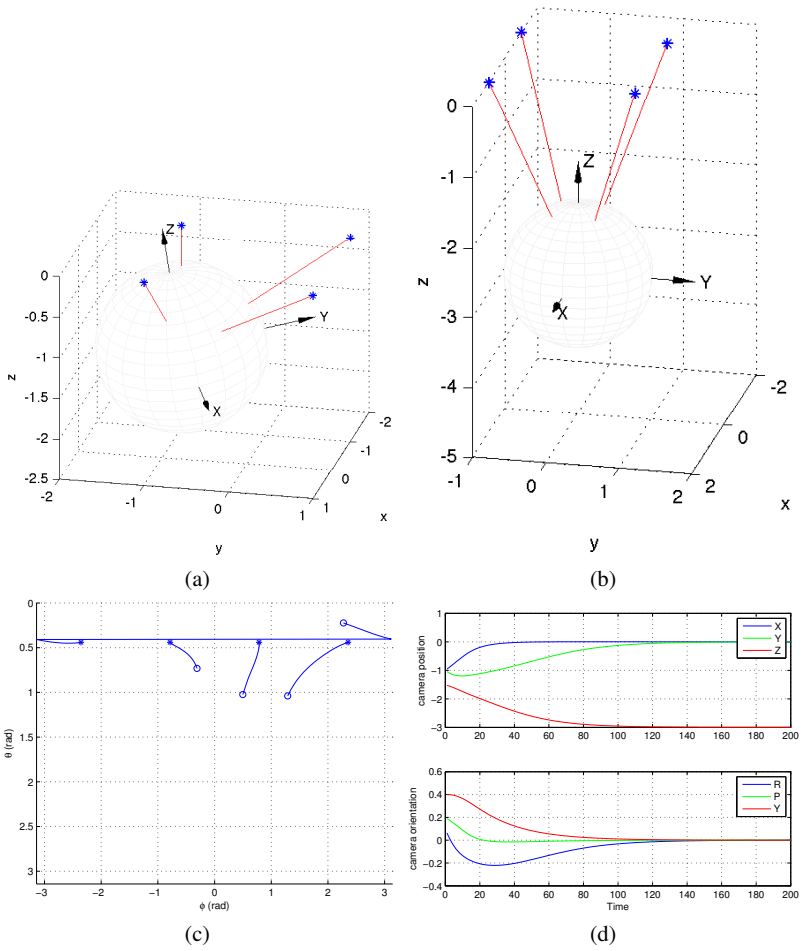

Fig. 6 IBVS on the sphere. (a) initial pose, (b) final pose, (c) feature motion on the θ-ϕ plane, (d) pose evolution.

be known apriori, the robot moves toward the observed target wherever it might be in the workspace. Image-based control can be considered as an inverse problem to optical flow — given a current and desired view the required optical flow can be computed, the problem is to determine the motion in SE(3) to achieve it. Most of the visual servoing literature is concerned with perspective cameras and a Cartesian image plane. More recently polar coordinates have been used with perspective cameras, and spherical cameras [17, 22].

For control purposes we follow the normal procedure of computing one 2×6 Jacobian, (9), for each of N feature points and stacking them to form a $2N \times 6$ matrix

$$\begin{bmatrix} \dot{\theta}_1 \\ \dot{\phi}_1 \\ \vdots \\ \dot{\theta}_N \\ \dot{\phi}_N \end{bmatrix} = \begin{bmatrix} \mathbf{J}_{\mathbf{p}_1} \\ \vdots \\ \mathbf{J}_{\mathbf{p}_N} \end{bmatrix} \mathbf{v} \tag{17}$$

The control law is

$$\mathbf{v} = \mathbf{J}^{+} \dot{f}^{*} \tag{18}$$

where $\dot{f}^{*}$ is the desired velocity of the features. Typically we choose this to be proportional to feature error

$$\dot{f}^{*} = -\gamma(f \ominus f^{*}) \tag{19}$$

where γ is a positive gain, f is the current value of the feature vector, and f^{*} is the desired value, which leads to linear motion of features within the feature space. $\ominus$ denotes modulo subtraction giving the smallest angular distance given that $\theta = [0,\ \pi)$ and $\phi = [-\pi,\ \pi)$.

Figure 6 presents simulation results for spherical IBVS for the case of general motion with translation and rotation in all axes. The target consists of four points arranged in the plane, and the servo task is to move to a pose where the camera's z-axis is normal to the plane and 3 m away. We can see that the velocity demand is well behaved and that the features have followed direct paths in the feature space. One feature has wrapped around in the azimuth direction.

If the attitude was servoed by a non-visual sensor such as gyroscope, accelerometer or magnetometer then we could use a partitioned IBVS scheme [10] where we would write (11) as

$$\frac{1}{Z}\mathbf{J}_t(\theta, \phi) \begin{bmatrix} t_x \\ t_y \\ t_z \end{bmatrix} = \begin{bmatrix} \dot{\theta} \\ \dot{\phi} \end{bmatrix} - \mathbf{J}_\omega(\theta, \phi) \begin{bmatrix} \omega_x \\ \omega_y \\ \omega_z \end{bmatrix} \tag{20}$$

and solve for translational velocity.

Classical visual servo control, as just described was principally developed for serial-link robotic manipulators [21] where all camera degrees of freedom are actuated. The dynamics of the system are easily compensated using a computed torque (or high gain) control design and the visual servo control may be derived from a first order model of the image dynamics [14]. Recent applications in high performance systems and under-actuated dynamic systems have lead researchers to consider full dynamic control design. Coupling of the camera ego-motion dynamics in the image plane proves to be a significant obstacle in achieving this goal and [24] proposed an asymptotically stable method for position regulation for fixed-camera visual servoing for a dynamic system. A further complication is encountered when an under-actuated dynamic system is used as the platform for the camera and [40] used a Lagrangian representation of the system dynamics to obtain an IBVS control for a blimp, an under-actuated, non-holonomic system.

An IBVS controller for a class of under-actuated dynamic systems has been proposed [17]that does not require accurate depth information for image features. Exploiting passivity they observe that

> *the only image geometry that preserves the passivity-like properties of the body fixed frame dynamics of a rigid object in the image space are those of a spherical camera.*

6 Structure and motion estimation on the sphere

In the IBVS example of the previous section the values of Z required to compute the image Jacobian were taken from the simulation engine, but in a real system they would not be known. Experience with IBVS shows that it is quite robust to errors in point depth, Z, and typically the final depth value is assumed throughout the motion.

The point depth can also be estimated, by rewriting (11) in identification form as

$$\left(\mathbf{J}_t(\theta, \phi) \begin{bmatrix} t_x \\ t_y \\ t_z \end{bmatrix} \right) (1/Z) = \begin{bmatrix} \dot{\theta} \\ \dot{\phi} \end{bmatrix} - \mathbf{J}_\omega(\theta, \phi) \begin{bmatrix} \omega_x \\ \omega_y \\ \omega_z \end{bmatrix} \tag{21}$$

or

$$\mathbf{A}\theta = \mathbf{b} \tag{22}$$

where the camera motion $(T_x,\ T_y,\ T_z,\ \omega_x,\ \omega_y,\ \omega_z)$ is known, since IBVS commands it, and $(\dot{\theta},\ \dot{\phi})$ is the optical flow which is observed during the motion. This a spherical structure from motion (SfM) system [20]. For the example of the previous section, the results of this estimator are shown in Figure 7 for one of the four target points. This is a very cheap estimator but we could also use a Kalman filter as is of-

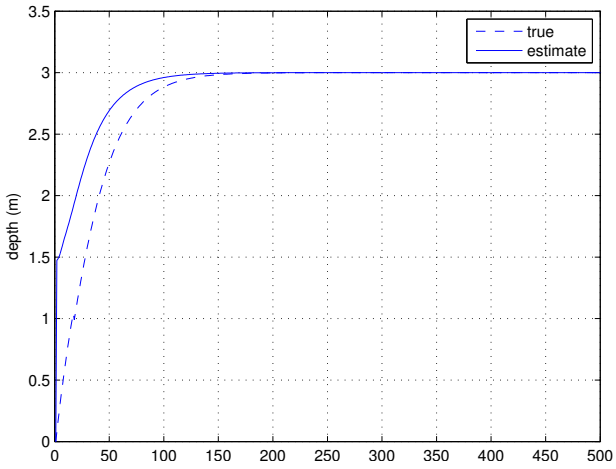

Fig. 7 Comparison of estimated and true point depth.

ten used in structure from motion systems. Depth could be estimated for all tracked points in the scene, not just those used for servoing.

This leads to our final use for the sphere, the scene structure can be conveniently considered in camera-centric form as a spherical depth map $D : \mathbb{S}^2 \rightarrow \mathbb{R}$. This form makes it trivially easy to handle camera rotational motion, the depth map rolls around the sphere. For translational motion of the camera points move over the sphere according to the direction of translation and point depth. We believe that this structure is amenable to a particle filter, operating on the sphere, which is able to better model the non-Gaussian distribution of depth uncertainty.

7 Conclusions

In this paper we have presented the sphere as a unifying concept, not just for cameras, but for sensor fusion, estimation and control. For robots that move in $SE(3)$ such as UAVs or AUVs the advantages of the sphere are particularly strong.

The unified imaging model is of Geyer and Daniilidas [16] is well known and uses spherical projection to model catadioptric cameras with mirrors which are conics. However the model is also an excellent approximation for other shaped mirrors such as equiangular and can also model many fisheye lenses. This is convenient for robotics where the advantages of wide-angle cameras include wide perceptual field for path planning and collision avoidance and resolving the ambiguity between rotation and translation which is problematic in a perspective cameras. The unified model also provides a framework for mosaic creation through projection from camera image planes, and image processing operations such as scale-space feature detectors can be formulated on the sphere. Camera ego-motion results in the apparent motion of points, optical flow, in the spherical image. Points on the surface of a sphere are commonly described by a unit 3-vector but this description is redundant and we presented a formulation of the optical flow equation in terms of two angles: colatitude and azimuth. spherical imaging model are increasingly well known.

The problem of attitude estimation is very naturally treated on the sphere using the matrix Lie-group representation of $SO(3)$. An asymptotically stable estimator that can incorporate multiple sensors such as gyroscopes, magnetometers, accelerometers and visual landmarks is presented. Inverting the optical flow equation leads to a spherical image-based visual servoing scheme which exhibits the desirable properties of the more well-known planar IBVS scheme such as robustness to depth uncertainty, and like the polar-planar IBVS performs well for large rotational motions. Adding a simple state estimator based on the inverted optical flow equation leads to a structure from motion solution, and the consideration of a camera-centric spherical depth map as a convenient world representation.

References

1. Baerveldt, A.J., Klang, R.: A low-cost and low-weight attitude estimation system for an autonomous helicopter. Intelligent Engineering Systems (1997)
2. Bonnabel, S., Martin, P., Rouchon, P.: Invariant asymptotic observers. IEEE Transactions on Automatic Control (2008). URL http://arxiv.org/abs/math.OC/0612193. Accepted for publication
3. Bülow, T.: Spherical diffusion for 3D surface smoothing. IEEE Transactions on Pattern Analysis and Machine Intelligence **26**(12), 1650–1654 (2004)
4. Campoloa, D., Kellerb, F., Guglielmellia, E.: Inertial/magnetic sensors based orientation tracking on the group of rigid body rotations with application to wearable devices. In: Proceedings of the 2006 IEEE/RSJ International Conference on Intelligent Robots and Systems, pp. 4762–4767. Beijing, China (2006)
5. Chahl, J.S., Srinivasan, M.V.: Reflective surfaces for panoramic imaging. Applied Optics (36), 8275–8285 (1997)
6. Chahl, J.S., Thakoor, S., Bouffant, N.L., Stange, G., Srinivasan, M.V., Hine, B., Zornetzer, S.: Bioinspired engineering of exploration systems: A horizon sensor/attitude reference system based on the dragonfly ocelli for mars exploration applications. J. Field Robotics **20**(1), 35–42 (2003)
7. Chaumette, F., Hutchinson, S.: Visual servo control. i. basic approaches. Robotics & Automation Magazine, IEEE **13**(4), 82–90 (2006). DOI 10.1109/MRA.2006.250573
8. Chaumette, F., Hutchinson, S.: Visual servo control. ii. advanced approaches [tutorial]. Robotics & Automation Magazine, IEEE **14**(1), 109–118 (2007). DOI 10.1109/MRA.2007.339609
9. Corke, P.: An inertial and visual sensing system for a small autonomous helicopter. J. Robotic Systems **21**(2), 43–51 (2004)
10. Corke, P., Hutchinson, S.A.: A new partitioned approach to image-based visual servo control. IEEE Trans. Robot. Autom. **17**(4), 507–515 (2001)
11. Corke, P., Lobo, J., Dias, J.: An introduction to inertial and visual sensing. Int. J. Robotics Research **26**(6), 519–536 (2007)
12. Corke, P., Strelow, D., Singh, S.: Omnidirectional visual odometry for a planetary rover. In: Proceedings International Conference on Intelligent Robots and Systems, pp. 4007–4012 (2004)
13. Crassidis, J.L., Markley, F.L., Cheng, Y.: Nonlinear attitude filtering methods. Journal of Guidance, Control,and Dynamics **30**(1), 12–28 (2007)
14. Espiau, B., Chaumette, F., Rives, P.: A new approach to visual servoing in robotics. IEEE Transactions on Robotics and Automation **8**(3), 313–326 (1992)
15. Gebre-Egziabher, D., Hayward, R., Powell, J.: Design of multi-sensor attitude determination systems. IEEE Transactions on Aerospace and Electronic Systems **40**(2), 627–649 (2004)
16. Geyer, C., Daniilidis, K.: A unifying theory for central panoramic systems and practical implications. In: Proceedings European Conference on Computer Vision (2000)
17. Hamel, T., Mahony, R.: Visual servoing of an under-actuated dynamic rigid-body system: An image based approach. IEEE Transactions on Robotics and Automation **18**(2), 187–198 (2002)
18. Hansen, P., Boles, W., Corke, P.: Spherical diffusion for scale-invariant keypoint detection in wide-angle images. In: DICTA '08: Proceedings of the 2008 Digital Image Computing: Techniques and Applications, pp. 525–532 (2008)
19. Hatch, R.: Synergism of gps code and carrier measurements. In: Proceedings of the 3rd International Geodetic Sypomsium on Satellite Doppler Positioning, vol. 2, pp. 1213–1232. Las Cruces, New Mexico (1982)
20. Huang, T., Netravali, A.: Motion and structure from feature correspondences: a review. Proceedings of the IEEE **82**(2), 252–268 (1994). DOI 10.1109/5.265351
21. Hutchinson, S., Hager, G., Corke, P.: A tutorial on visual servo control. IEEE Transactions on Robotics and Automation **12**(5), 651–670 (1996)

22. Iwatsuki, M., Okiyama, N.: A new formulation of visual servoing based on cylindrical coordinate system with shiftable origin. In: Intelligent Robots and System, 2002. IEEE/RSJ International Conference on, vol. 1, pp. 354–359 vol.1 (2002). DOI 10.1109/IRDS.2002.1041414
23. Jun, M., Roumeliotis, S., Sukhatme, G.: State estimation of an autonomous helicopter using Kalman filtering. In: Proc. 1999 IEEE/RSJ International Conference on Robots and Systems (IROS 99) (1999)
24. Kelly, R.: Robust asymptotically stable visual servoing of planar robots. IEEE Transactions on Robotics and Automation **12**(5), 759–766 (1996)
25. Krishnan, G., Nayar, S.K.: Towards a true spherical camera. In: Society of Photo-Optical Instrumentation Engineers (SPIE) Conference Series, *Society of Photo-Optical Instrumentation Engineers (SPIE) Conference Series*, vol. 7240 (2009). DOI 10.1117/12.817149
26. Lefferts, E., Markley, F., Shuster, M.: Kalman filtering for spacecraft attitude estimation. AIAA Journal of Guidance, Control and Navigation **5**(5), 417–429 (1982)
27. Lim, J., Barnes, N.: Directions of egomotion from antipodal points. In: CVPR. IEEE Computer Society (2008)
28. Lobo, J., Dias, J.: Vision and inertial sensor cooperation using gravity as a vertical reference. IEEE Transactions on Pattern Analysis and Machine Intelligence **25**(12), 1597–1608 (2003)
29. Mahony, R., Hamel, T., Pflimlin, J.M.: Non-linear complementary filters on the special orthogonal group. IEEE Transactions on Automatic Control **53**(5), 1203–1218 (2008). Digital Object Identifier 10.1109/TAC.2008.923738
30. Martin, P., Salaün, E.: An invariant observer for earth-velocity-aided attitude heading reference systems. In: Proceedings of the 17th World Congress The International Federation of Automatic Control. Seoul, Korea, (2008)
31. Nayar, S.K.: Catadioptric omnidirectional camera. Computer Vision and Pattern Recognition, IEEE Computer Society Conference on **0**, 482 (1997). DOI http://doi.ieeecomputersociety.org/10.1109/CVPR.1997.609369
32. Roberts, J.M., Corke, P.I., Buskey, G.: Low-cost flight control system for small autonomous helicopter. In: Australian Conference on Robotics and Automation, Auckland, 27-29 Novembre, pp. 71–76 (2002)
33. Schill, F., Mahony, R., Corke, P., Cole, L.: Virtual force feedback teleoperation of the insectbot using optical flow. In: J. Kim, R. Mahony (eds.) Proc. Australian Conf. Robotics and Automation (2008). URL http://www.araa.asn.au/acra/acra2008/papers/pap159s1.pdf
34. Strelow, D., Mishler, J., Koes, D., Singh, S.: Precise omnidirectional camera calibration. Computer Vision and Pattern Recognition, IEEE Computer Society Conference on **1**, 689 (2001). DOI http://doi.ieeecomputersociety.org/10.1109/CVPR.2001.990542
35. Sukhatme, G.S., Roumeliotis, S.I.: State estimation via sensor modeling for helicopter control using an indirect Kalman filter. In: Int.Conf. Intelligent Robotics (IROS) (1999)
36. Tahri, O., Mezouar, Y., Chaumette, F., Corke, P.: Generic decoupled image-based visual servoing for cameras obeying the unified projection model. In: icra, p. accepted (2009)
37. Vasconcelos, J., Silvestre, C., Oliveira, P.: A nonlinear observer for rigid body attitude estimation using vector observations. In: Proceedings of the 17th World Congress The International Federation of Automatic Control, pp. 8599–8604. Seoul, Korea, (2008)
38. Vik, B., Fossen, T.: A nonlinear observer for GPS and INS integration. In: Proc. IEEE Conf. on Decisioin and Control, pp. 2956–2961 (2001)
39. Ying, X., Hu, Z.: Can we consider central catiodioptric cameras and fisheye cameras within a unified imaging model. In: 8th European Conference on Computer Vision, pp. 442–455 (2004)
40. Zhang, H., Ostrowski, J.P.: Visual servoing with dynamics: Control of an unmanned blimp. In: Proceedings of the IEEE Internation Conference on Robotics and Automation, pp. 618–623. Detroit, Michigan, U.S.A. (1999)